Photoproduction in Ultra-Peripheral Relativistic Heavy Ion Collisions at STAR

Boris Grube

Pusan National University, Department of Physics
Busan, Republic of Korea

Brookhaven National Laboratory
Upton, NY, U.S.A.

for the STAR Collaboration

Workshop on High Energy Photon Collisions at the LHC
CERN, Geneva
23rd April 2008

PUSAN NATIONAL UNIVERSITY

BROOKHAVEN NATIONAL LABORATORY

Outline

1. Introduction
   - Ultra-peripheral relativistic heavy ion collisions at STAR
   - Experimental setup
   - Triggering and data selection
2. Results on photonuclear ρ production in Au $\times$ Au collisions
   - ρ production cross section
   - Spin structure of ρ production amplitudes
   - Interference effects in coherent ρ production
3. Other results
   - Photonuclear ρ production in d $\times$ Au collisions
   - $\pi^+\pi^-\pi^+\pi^-$ production in Au $\times$ Au collisions
   - e^+e^--pair production in Au $\times$ Au collisions

Outline

Ultra-Peripheral Heavy Ion Collisions (UPC) at STAR

UPC processes measured at STAR

1. **Photonuclear interactions**
   - ρ production in Au $\times$ Au @ $\sqrt{s_{NN}} = 200$, and 130 GeV
   - γ^* from "spectator" ion fluctuates into $q\bar{q}$-pair
   - $q\bar{q}$-pair scatters off "target" nucleus into real vector meson
   - Scattering described in terms of soft Pomeron exchange

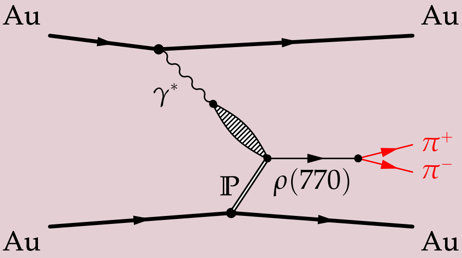

Ultra-Peripheral Heavy Ion Collisions (UPC) at STAR

UPC processes measured at STAR (cont.)

2. **Photonuclear interactions with mutual nuclear breakup**
   - ρ production in Au $\times$ Au @ $\sqrt{s_{NN}} = 200, 130$, and $62\,\mathrm{GeV}$
   - Mutual Coulomb excitation of nuclei by additional photons
     - Independent of meson production
     - Predominantly excitation of Giant Dipole Resonance (GDR)
     - GDRs decay via neutron emission $\Longrightarrow$ distinctive signature

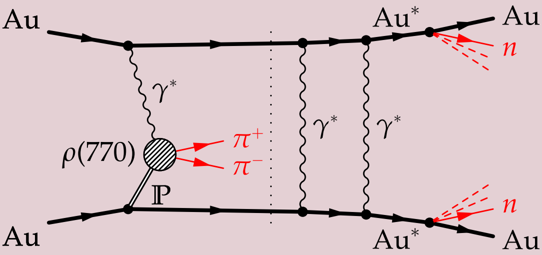

Ultra-Peripheral Heavy Ion Collisions (UPC) at STAR

UPC processes measured at STAR (cont.)

2. **Photonuclear interactions with mutual nuclear breakup**
   - ρ production in Au $\times$ Au @ $\sqrt{s_{NN}} = 200, 130$, and 62 GeV
   - Mutual Coulomb excitation of nuclei by additional photons
     - Independent of meson production
     - Predominantly excitation of Giant Dipole Resonance (GDR)
     - GDRs decay via neutron emission $\Longrightarrow$ distinctive signature

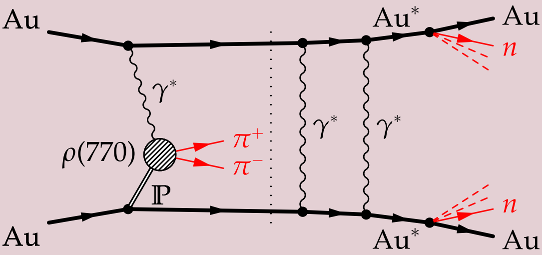

Ultra-Peripheral Heavy Ion Collisions (UPC) at STAR

UPC processes measured at STAR (cont.)

3. **Photon-photon interactions with mutual nuclear breakup**
   - e^+e^--pair production in Au $\times$ Au @ $\sqrt{s_{NN}} = 200\,\text{GeV}$

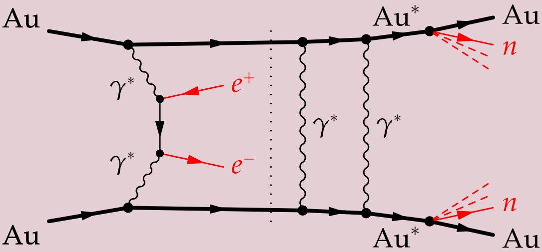

The STAR Experiment at RHIC

Detector components important for UPC measurements Nucl. Instr. Meth. **A499**

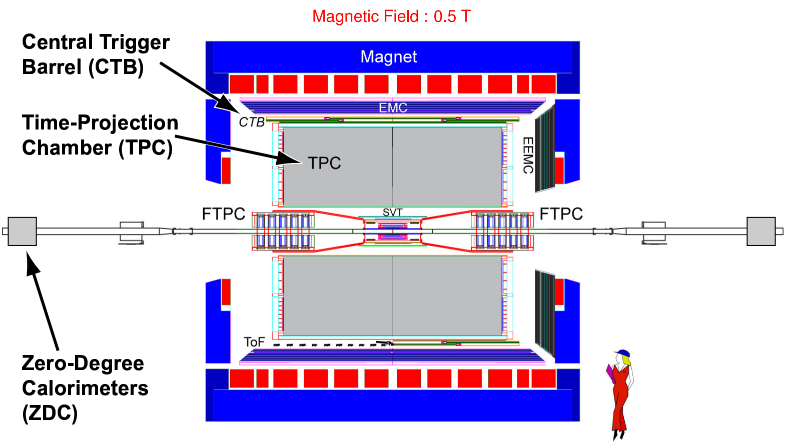

Triggering and Data Selection

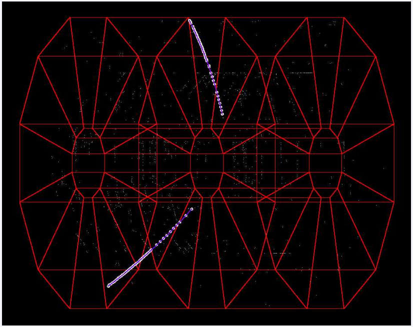

TPC tracks for typical ρ event

Experimental signature and event selection

- Coherent production dominates: particles produced in $\gamma^*\gamma^*$ and $\gamma^*\mathbb{P}$ have low $p_T \lesssim 2\hbar/R_A \approx 60$ MeV/c
- 2 well reconstructed tracks
  - From common vertex
  - Opposite charge
  - Low net p_T
- Vertex position close to interaction diamond
- Low overall track multiplicity
- For nuclear breakup: additional forward neutrons $\Longrightarrow$ trigger

STAR acceptance limits accessible rapidities to $|y| < 1$

Triggering and Data Selection

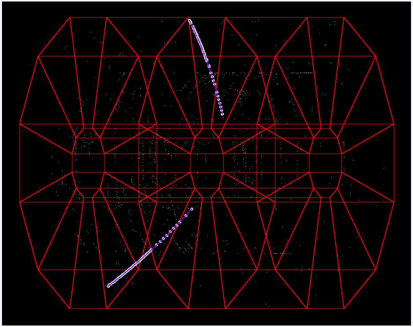

TPC tracks for typical ρ event

Experimental signature and event selection

- Coherent production dominates: particles produced in $\gamma^*\gamma^*$ and $\gamma^*\mathbb{P}$ have low $p_T \lesssim 2\hbar/R_A \approx 60\ \mathrm{MeV}/c$
- 2 well reconstructed tracks
  - From common vertex
  - Opposite charge
  - Low net p_T
- Vertex position close to interaction diamond
- Low overall track multiplicity
- For nuclear breakup: additional forward neutrons $\Longrightarrow$ trigger

STAR acceptance limits accessible rapidities to $|y| < 1$

Triggering and Data Selection

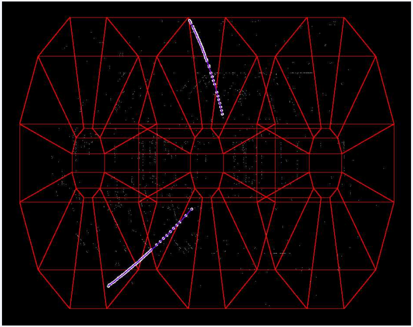

TPC tracks for typical ρ event

Experimental signature and event selection

- Coherent production dominates: particles produced in $\gamma^*\gamma^*$ and $\gamma^*\mathbb{P}$ have low $p_T \lesssim 2\hbar/R_A \approx 60$ MeV/c
- 2 well reconstructed tracks
  - From common vertex
  - Opposite charge
  - Low net p_T
- Vertex position close to interaction diamond
- Low overall track multiplicity
- For nuclear breakup: additional forward neutrons $\Longrightarrow$ trigger

STAR acceptance limits accessible rapidities to $|y| < 1$

Triggering and Data Selection

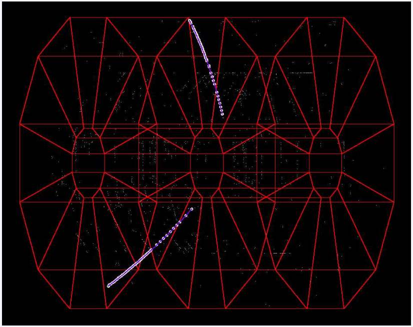

TPC tracks for typical ρ event

Experimental signature and event selection

- Coherent production dominates: particles produced in $\gamma^*\gamma^*$ and $\gamma^*\mathbb{P}$ have low $p_T \lesssim 2\hbar/R_A \approx 60$ MeV$/c$
- 2 well reconstructed tracks
  - From common vertex
  - Opposite charge
  - Low net p_T
- Vertex position close to interaction diamond
- Low overall track multiplicity
- For nuclear breakup: additional forward neutrons $\Longrightarrow$ trigger

STAR acceptance limits accessible rapidities to $|y| < 1$

UPC Triggers

2 triggers used at STAR

1. **Topology trigger** (CTB only)
   - CTB is subdivided into 4 quadrants
   - Top+Bottom quadrants veto cosmic rays
   - Coincidence of North and South quadrants
   - In addition low multiplicity requirement
   - **Does not require nuclear breakup**

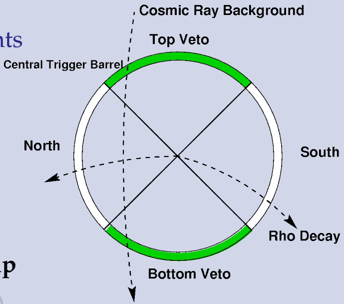

2. **Minimum bias trigger** (ZDC only)
   - Coincident neutrons in both ZDCs

UPC Triggers

2 triggers used at STAR

1. **Topology trigger** (CTB only)
   - CTB is subdivided into 4 quadrants
   - Top+Bottom quadrants veto cosmic rays
   - Coincidence of North and South quadrants
   - In addition low multiplicity requirement
   - **Does not require nuclear breakup**
2. **Minimum bias trigger** (ZDC only)
   - Coincident neutrons in both ZDCs

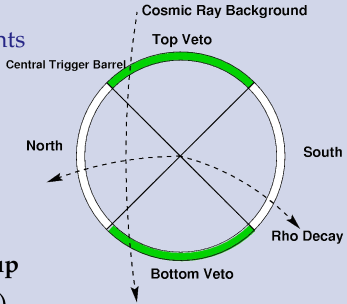

Triggering and Data Selection

Main background contributions

1. **Beam-gas interactions** reduced by
   - Requiring low track multiplicity
   - Limiting primary vertex position
2. **Peripheral hadronic interactions** reduced by
   - Requiring low track multiplicity
   - Selecting low p_T
3. **Pile-up events** reduced by
   - Requiring low track multiplicity
   - Limiting primary vertex position
4. **Cosmic rays** reduced by
   - Limiting primary vertex position
   - Minimum bias trigger: ZDC neutron tag
   - Topology trigger: excluding events close to $|y| = 0$

Triggering and Data Selection

Main background contributions

1. **Beam-gas interactions** reduced by
   - Requiring low track multiplicity
   - Limiting primary vertex position
2. **Peripheral hadronic interactions** reduced by
   - Requiring low track multiplicity
   - Selecting low p_T
3. **Pile-up events** reduced by
   - Requiring low track multiplicity
   - Limiting primary vertex position
4. **Cosmic rays** reduced by
   - Limiting primary vertex position
   - Minimum bias trigger: ZDC neutron tag
   - Topology trigger: excluding events close to $|y| = 0$

Triggering and Data Selection

Main background contributions

1. **Beam-gas interactions** reduced by
   - Requiring low track multiplicity
   - Limiting primary vertex position
2. **Peripheral hadronic interactions** reduced by
   - Requiring low track multiplicity
   - Selecting low p_T
3. **Pile-up events** reduced by
   - Requiring low track multiplicity
   - Limiting primary vertex position
4. **Cosmic rays** reduced by
   - Limiting primary vertex position
   - Minimum bias trigger: ZDC neutron tag
   - Topology trigger: excluding events close to $|y| = 0$

Triggering and Data Selection

Main background contributions

1. **Beam-gas interactions** reduced by
   - Requiring low track multiplicity
   - Limiting primary vertex position
2. **Peripheral hadronic interactions** reduced by
   - Requiring low track multiplicity
   - Selecting low p_T
3. **Pile-up events** reduced by
   - Requiring low track multiplicity
   - Limiting primary vertex position
4. **Cosmic rays** reduced by
   - Limiting primary vertex position
   - Minimum bias trigger: ZDC neutron tag
   - Topology trigger: excluding events close to $|y| = 0$

Triggering and Data Selection

Main background contributions

1. **Beam-gas interactions** reduced by
   - Requiring low track multiplicity
   - Limiting primary vertex position
2. **Peripheral hadronic interactions** reduced by
   - Requiring low track multiplicity
   - Selecting low p_T
3. **Pile-up events** reduced by
   - Requiring low track multiplicity
   - Limiting primary vertex position
4. **Cosmic rays** reduced by
   - Limiting primary vertex position
   - Minimum bias trigger: ZDC neutron tag
   - Topology trigger: excluding events close to $|y| = 0$

Outline

ρ Yield from Run 2 Au $\times$ Au @ $\sqrt{s_{NN}} = 200$ GeV

2 trigger sets

1. **Topology trigger**
   - No nuclear breakup required
   - $13\,054 \pm 124$ ρ candidates
2. **Minimum bias trigger**
   - ZDC neutron tag
   - $3\,075 \pm 128$ ρ candidates

- Background estimate from like-sign pairs $\pi^\pm\pi^\pm$

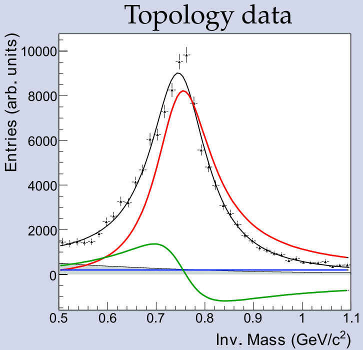

PR **C77**, 034910 (2008)

ρ Yield from Run 2 Au $\times$ Au @ $\sqrt{s_{NN}} = 200\,\text{GeV}$

2 trigger sets

1. **Topology trigger**
   - No nuclear breakup required
   - $13\,054 \pm 124$ ρ candidates
2. **Minimum bias trigger**
   - ZDC neutron tag
   - $3\,075 \pm 128$ ρ candidates

- Background estimate from like-sign pairs $\pi^{\pm}\pi^{\pm}$

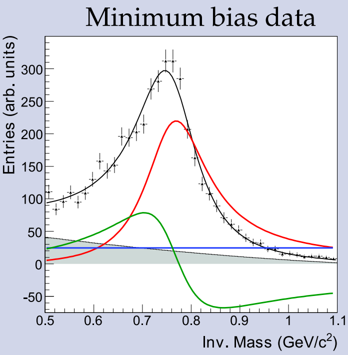

PR **C77**, 034910 (2008)

ρ Yield from Run 2 Au $\times$ Au @ $\sqrt{s_{NN}} = 200\,\text{GeV}$

2 trigger sets

1. **Topology trigger**
   - No nuclear breakup required
   - $13\,054 \pm 124$ ρ candidates
2. **Minimum bias trigger**
   - ZDC neutron tag
   - $3\,075 \pm 128$ ρ candidates

- Background estimate from like-sign pairs $\pi^{\pm}\pi^{\pm}$

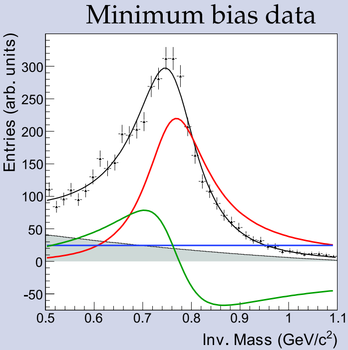

PR **C77**, 034910 (2008)

ρ Invariant Mass Fit

Fit function with 4 components

$$\frac{d\sigma}{dM_{\pi\pi}} = \left| A \frac{\sqrt{M_{\pi\pi} M_\rho \Gamma}}{M_{\pi\pi}^2 - M_\rho^2 + i M_\rho \Gamma} + B \right|^2 + f_{BG}$$

$$\text{with } \Gamma(M_{\pi\pi}) \equiv \Gamma_\rho \frac{M_\rho}{M_{\pi\pi}} \left[\frac{M_{\pi\pi}^2 - 4m_\pi^2}{M_\rho^2 - 4m_\pi^2} \right]^{\frac{3}{2}}$$

Minimum bias data

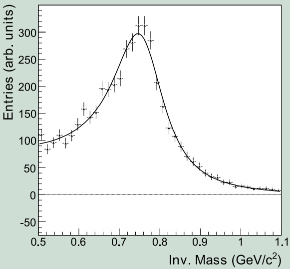

1. Relativistic Breit-Wigner function for ρ peak with amplitude A
2. Constant direct $\pi^+\pi^-$ production amplitude B
3. Söding term for interference of the two
4. 2nd order polynomial f_{BG} describes background from like-sign pairs

ρ Invariant Mass Fit

Fit function with 4 components

$$\frac{d\sigma}{dM_{\pi\pi}} = \left| A \frac{\sqrt{M_{\pi\pi} M_\rho \Gamma}}{M_{\pi\pi}^2 - M_\rho^2 + iM_\rho\Gamma} + B \right|^2 + f_{BG}$$

$$\text{with } \Gamma(M_{\pi\pi}) \equiv \Gamma_\rho \frac{M_\rho}{M_{\pi\pi}} \left[\frac{M_{\pi\pi}^2 - 4m_\pi^2}{M_\rho^2 - 4m_\pi^2} \right]^{\frac{3}{2}}$$

1. Relativistic Breit-Wigner function for ρ peak with amplitude A
2. Constant direct $\pi^+\pi^-$ production amplitude B
3. Söding term for interference of the two
4. 2nd order polynomial f_{BG} describes background from like-sign pairs

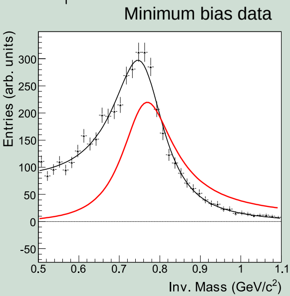

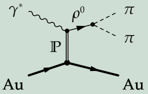

ρ Invariant Mass Fit

Fit function with 4 components

$$\frac{\mathrm{d}\sigma}{\mathrm{d}M_{\pi\pi}} = \left| A \frac{\sqrt{M_{\pi\pi} M_\rho \Gamma}}{M_{\pi\pi}^2 - M_\rho^2 + i M_\rho \Gamma} + B \right|^2 + f_{\mathrm{BG}}$$

$$\text{with } \Gamma(M_{\pi\pi}) \equiv \Gamma_\rho \frac{M_\rho}{M_{\pi\pi}} \left[\frac{M_{\pi\pi}^2 - 4m_\pi^2}{M_\rho^2 - 4m_\pi^2} \right]^{\frac{3}{2}}$$

1. Relativistic Breit-Wigner function for ρ peak with amplitude A
2. Constant direct $\pi^+\pi^-$ production amplitude B
3. Söding term for interference of the two
4. 2nd order polynomial f_{BG} describes background from like-sign pairs

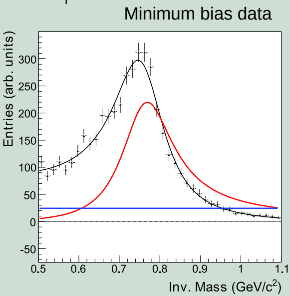

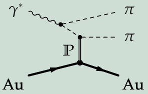

ρ Invariant Mass Fit

Fit function with 4 components

$$\frac{d\sigma}{dM_{\pi\pi}} = \left| A \frac{\sqrt{M_{\pi\pi} M_\rho \Gamma}}{M_{\pi\pi}^2 - M_\rho^2 + i M_\rho \Gamma} + B \right|^2 + f_{BG}$$

$$\text{with } \Gamma(M_{\pi\pi}) \equiv \Gamma_\rho \frac{M_\rho}{M_{\pi\pi}} \left[\frac{M_{\pi\pi}^2 - 4m_\pi^2}{M_\rho^2 - 4m_\pi^2} \right]^{\frac{3}{2}}$$

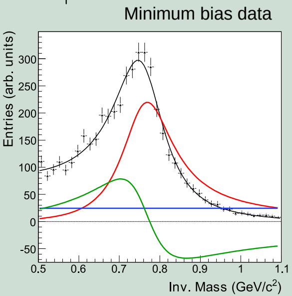

1. Relativistic Breit-Wigner function for ρ peak with amplitude A
2. Constant direct $\pi^+\pi^-$ production amplitude B
3. Söding term for interference of the two
4. 2nd order polynomial f_{BG} describes background from like-sign pairs

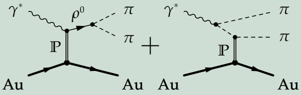

ρ Invariant Mass Fit

Fit function with 4 components

$$\frac{\mathrm{d}\sigma}{\mathrm{d}M_{\pi\pi}} = \left| A \frac{\sqrt{M_{\pi\pi} M_\rho \Gamma}}{M_{\pi\pi}^2 - M_\rho^2 + i M_\rho \Gamma} + B \right|^2 + f_{\mathrm{BG}}$$

$$\text{with } \Gamma(M_{\pi\pi}) \equiv \Gamma_\rho \frac{M_\rho}{M_{\pi\pi}} \left[\frac{M_{\pi\pi}^2 - 4m_\pi^2}{M_\rho^2 - 4m_\pi^2} \right]^{\frac{3}{2}}$$

1. Relativistic Breit-Wigner function for ρ peak with amplitude A
2. Constant direct $\pi^+\pi^-$ production amplitude B
3. Söding term for interference of the two
4. 2nd order polynomial f_{BG} describes background from like-sign pairs

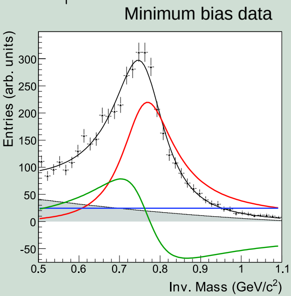

Direct $\pi^+\pi^-$ vs. ρ Production

Ratio of non-resonant to resonant $\pi^+\pi^-$ production

$$\frac{\mathrm{d}\sigma}{\mathrm{d}M_{\pi\pi}} = \left| A \frac{\sqrt{M_{\pi\pi}M_\rho\Gamma}}{M_{\pi\pi}^2 - M_\rho^2 + iM_\rho\Gamma} + B \right|^2 + f_{\mathrm{BG}}$$

- Amplitudes A and B are fit parameters
- B/A measure for ratio of non-resonant to resonant $\pi^+\pi^-$ production
  - For Au $\times$ Au @ $\sqrt{s_{NN}} = 200\,\mathrm{GeV}$: $|B/A| = 0.89 \pm 0.08_{\mathrm{stat.}} \pm 0.09_{\mathrm{syst.}}\,\mathrm{GeV}^{-\frac{1}{2}}$
  - No dependence on angles or rapidity

    PR **C77**, 034910 (2008)
  - For Au $\times$ Au @ $\sqrt{s_{NN}} = 130\,\mathrm{GeV}$: $|B/A| = 0.81 \pm 0.08_{\mathrm{stat.}} \pm 0.20_{\mathrm{syst.}}\,\mathrm{GeV}^{-\frac{1}{2}}$

    PRL **89**, 272302 (2002)
  - In agreement with ZEUS EPJ **C2**, 247 (1998)

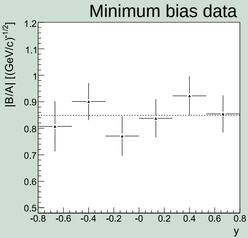

Direct $\pi^+\pi^-$ vs. ρ Production

Ratio of non-resonant to resonant $\pi^+\pi^-$ production

$$\frac{d\sigma}{dM_{\pi\pi}} = \left| A \frac{\sqrt{M_{\pi\pi} M_\rho \Gamma}}{M_{\pi\pi}^2 - M_\rho^2 + iM_\rho\Gamma} + B \right|^2 + f_{BG}$$

- Amplitudes A and B are fit parameters
- B/A measure for ratio of non-resonant to resonant $\pi^+\pi^-$ production
  - For Au $\times$ Au @ $\sqrt{s_{NN}} = 200\,\text{GeV}$:
    $|B/A| = 0.89 \pm 0.08_{\text{stat.}} \pm 0.09_{\text{syst.}}\ \text{GeV}^{-\frac{1}{2}}$
  - No dependence on angles or rapidity
    PR **C77**, 034910 (2008)
  - For Au $\times$ Au @ $\sqrt{s_{NN}} = 130\,\text{GeV}$:
    $|B/A| = 0.81 \pm 0.08_{\text{stat.}} \pm 0.20_{\text{syst.}}\ \text{GeV}^{-\frac{1}{2}}$
    PRL **89**, 272302 (2002)
  - In agreement with ZEUS EPJ **C2**, 247 (1998)

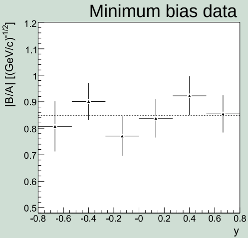

ρ Production Cross Section

Total ρ production cross section for Au $\times$ Au @ $\sqrt{s_{NN}} = 200$ GeV

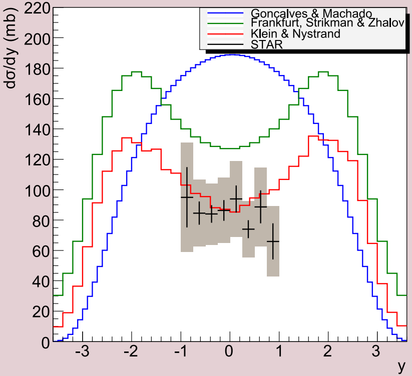

- σ_{tot} obtained by scaling σ_{mb}(nucl. breakup) from minimum bias data with ratio $\dfrac{\sigma_{\text{topo}}(\text{no nucl. breakup})}{\sigma_{\text{topo}}(\text{nucl. breakup})}$ from topology data

ρ Production Cross Section

Comparison with model predictions for Au $\times$ Au @ $\sqrt{s_{NN}} = 200$ GeV

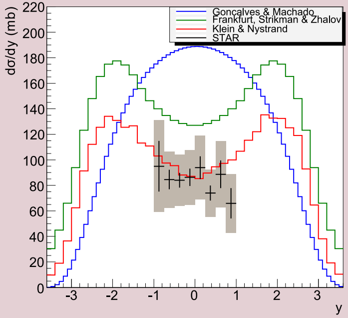

1. **Klein, Nystrand** PR **C60**, 014903 (1999)
   - Vector Dominance Model (VDM) for $\gamma^* \to |q\bar{q}\rangle$
   - Classical mechanical approach for scattering
   - Uses photoproduction data from $\gamma p \to \rho p$ experiments
2. **Frankfurt, Strikman, Zhalov** PR **C67**, 034901 (2003)
   - generalized VDM
   - QCD Gribov-Glauber approach
3. **Gonçalves, Machado** EPJ **C29**, 271-275 (2003)
   - QCD color dipole approach
   - Includes nuclear effects and parton saturation phenomena

ρ Production Cross Section

Comparison with model predictions for Au $\times$ Au @ $\sqrt{s_{NN}} = 200$ GeV

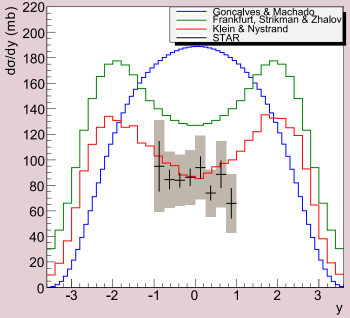

1. **Klein, Nystrand** PR **C60**, 014903 (1999)
   - Vector Dominance Model (VDM) for $\gamma^* \rightarrow |q\bar{q}\rangle$
   - Classical mechanical approach for scattering
   - Uses photoproduction data from $\gamma p \rightarrow \rho p$ experiments
2. **Frankfurt, Strikman, Zhalov** PR **C67**, 034901 (2003)
   - generalized VDM
   - QCD Gribov-Glauber approach
3. **Gonçalves, Machado** EPJ **C29**, 271-275 (2003)
   - QCD color dipole approach
   - Includes nuclear effects and parton saturation phenomena

ρ Production Cross Section

Comparison with model predictions for Au $\times$ Au @ $\sqrt{s_{NN}} = 200$ GeV

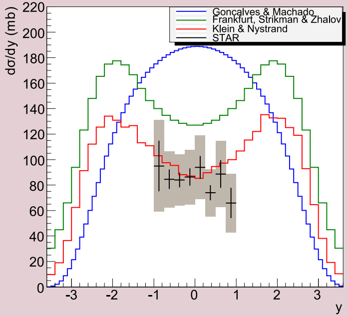

1. **Klein, Nystrand** PR **C60**, 014903 (1999)
   - Vector Dominance Model (VDM) for $\gamma^* \rightarrow |q\bar{q}\rangle$
   - Classical mechanical approach for scattering
   - Uses photoproduction data from $\gamma p \rightarrow \rho p$ experiments
2. **Frankfurt, Strikman, Zhalov** PR **C67**, 034901 (2003)
   - generalized VDM
   - QCD Gribov-Glauber approach
3. **Gonçalves, Machado** EPJ **C29**, 271-275 (2003)
   - QCD color dipole approach
   - Includes nuclear effects and parton saturation phenomena

ρ Production Cross Section

Energy dependence of coherent ρ production with nuclear breakup

- Based on total hadronic cross section of 7.2 b
- For **run 1** Au $\times$ Au @ $\sqrt{s_{NN}} = 130\,\text{GeV}$
  $\sigma_{XnXn}^{\text{coh}} = 28.3 \pm 2.0_{\text{stat.}} \pm 6.3_{\text{syst.}}\,\text{mb}$ PRL **89**, 272302 (2002)
- For **run 2** Au $\times$ Au @ $\sqrt{s_{NN}} = 200\,\text{GeV}$
  $\sigma_{XnXn}^{\text{coh}} = 31.9 \pm 1.5_{\text{stat.}} \pm 4.5_{\text{syst.}}\,\text{mb}$ PR **C77**, 034910 (2008)
- Currently analyzing **run 4**
  Au $\times$ Au @ $\sqrt{s_{NN}} = 62\,\text{GeV}$
  data to get third data point

ρ Production Cross Section

Energy dependence of coherent ρ production with nuclear breakup

- Based on total hadronic cross section of 7.2 b
- For **run 1** Au $\times$ Au @ $\sqrt{s_{NN}} = 130$ GeV
  $\sigma^{\text{coh}}_{XnXn} = 28.3 \pm 2.0_{\text{stat.}} \pm 6.3_{\text{syst.}}$ mb — PRL **89**, 272302 (2002)
- For **run 2** Au $\times$ Au @ $\sqrt{s_{NN}} = 200$ GeV
  $\sigma^{\text{coh}}_{XnXn} = 31.9 \pm 1.5_{\text{stat.}} \pm 4.5_{\text{syst.}}$ mb — PR **C77**, 034910 (2008)
- Currently analyzing **run 4**
  Au $\times$ Au @ $\sqrt{s_{NN}} = 62$ GeV
  data to get third data point

Minimum bias data

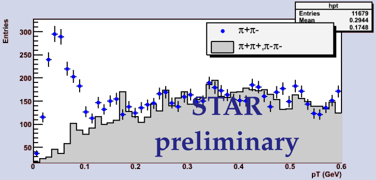

Spin Structure of ρ Production Amplitudes

Extraction of spin density matrix elements from $\pi^+\pi^-$ angular distribution

Schilling, Wolf NP **B61**, 381 (1973)

$$\frac{1}{\sigma}\frac{\mathrm{d}^2\sigma}{\mathrm{d}\cos\theta\,\mathrm{d}\phi} = \frac{3}{4\pi}\left[\frac{1}{2}(1 - r^{04}_{00}) + \frac{1}{2}(3r^{04}_{00} - 1)\cos^2\theta\right.$$
$$\left. - \sqrt{2}\,\Re\mathfrak{e}[r^{04}_{10}]\,\sin 2\theta\,\cos\phi - r^{04}_{1\,-1}\,\sin^2\theta\,\cos 2\phi\right]$$

- ρ production plane difficult to reconstruct
- Approximate production plane using beam direction
  - θ is polar angle between beam direction and $\vec{p}_{\pi^+}$ in ρ RF
  - ϕ is angle between ρ decay and production plane (w.r.t. beam)
- Due to ambiguity in beam direction cannot measure $\Re\mathfrak{e}[r^{04}_{10}]$ (interference between helicity non-flip and single-flip)

Spin Structure of ρ Production Amplitudes

Spin density matrix elements from fit of 2D angular distributions

1D projections of 2D angular distribution (minimum bias data)

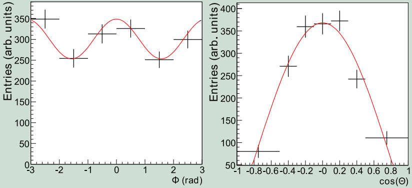

Parameter	STAR	ZEUS
r^{04}_{00}	$-0.03 \pm 0.03_{\text{stat.}} \pm 0.06_{\text{syst.}}$	$0.01 \pm 0.01_{\text{stat.}} \pm 0.02_{\text{syst.}}$
$\mathfrak{Re}[r^{04}_{10}]$	—	$0.01 \pm 0.01_{\text{stat.}} \pm 0.01_{\text{syst.}}$
r^{04}_{1-1}	$-0.01 \pm 0.03_{\text{stat.}} \pm 0.05_{\text{syst.}}$	$-0.01 \pm 0.01_{\text{stat.}} \pm 0.01_{\text{syst.}}$

- Results similar to ZEUS measurements EPJ **C2**, 247 (1998)
- Spin density elements close to zero indicate s-channel helicity conservation

Spin Structure of ρ Production Amplitudes

Spin density matrix elements from fit of 2D angular distributions

1D projections of 2D angular distribution (minimum bias data)

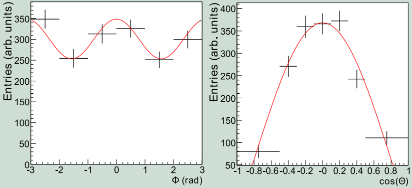

Parameter	STAR	ZEUS
r^{04}_{00}	$-0.03 \pm 0.03_{\text{stat.}} \pm 0.06_{\text{syst.}}$	$0.01 \pm 0.01_{\text{stat.}} \pm 0.02_{\text{syst.}}$
$\Re\mathfrak{e}[r^{04}_{10}]$	—	$0.01 \pm 0.01_{\text{stat.}} \pm 0.01_{\text{syst.}}$
$r^{04}_{1\,-1}$	$-0.01 \pm 0.03_{\text{stat.}} \pm 0.05_{\text{syst.}}$	$-0.01 \pm 0.01_{\text{stat.}} \pm 0.01_{\text{syst.}}$

- Results similar to ZEUS measurements EPJ **C2**, 247 (1998)
- Spin density elements close to zero indicate s-channel helicity conservation

Interference Effects in Coherent ρ Production

2-source interferometer

- Cannot distinguish γ^* source and target
- ρ production occurs close ($d \lesssim 1\,\mathrm{fm}$) to target nucleus

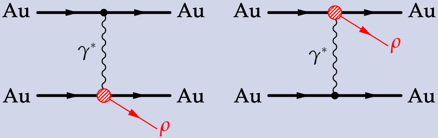

- Interference creates entangled final state $\pi^+\pi^-$ wave function
- $\mathbb{P}(\rho) = -1$: subtract amplitudes
  $$\sigma = \left| A(b,y) - A(b,-y)\, e^{i\vec{p}_T\cdot\vec{b}} \right|^2$$
- For $y \approx 0$: $A(b,y) \approx A(b,-y)$
  $$\Longrightarrow \quad \sigma = \sigma_0 \left[1 - \cos(\vec{p}_T \cdot \vec{b}) \right]$$
- Suppression at low $p_T \lesssim \hbar / \langle b \rangle$

Klein *et al.*, PL **A308**, 323 (2003)

Interference Effects in Coherent ρ Production

2-source interferometer

- Cannot distinguish γ^* source and target
- ρ production occurs close ($d \lesssim 1\,\text{fm}$) to target nucleus

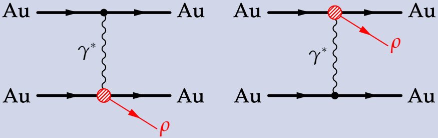

- Interference creates entangled final state $\pi^+\pi^-$ wave function
- $\mathbb{P}(\rho) = -1$: subtract amplitudes

$$\sigma = \left| A(b,y) - A(b,-y)\, e^{i\vec{p}_T\cdot\vec{b}} \right|^2$$

- For $y \approx 0$: $A(b,y) \approx A(b,-y)$

$$\implies \sigma = \sigma_0 \left[1 - \cos(\vec{p}_T \cdot \vec{b}) \right]$$

- Suppression at low $p_T \lesssim \hbar / \langle b \rangle$

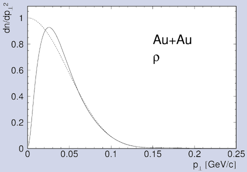

Klein *et al.*, PL **A308**, 323 (2003)

Interference Effects in Coherent ρ Production

Measuring interference in run 2 Au $\times$ Au @ $\sqrt{s_{NN}} = 200$ GeV collisions

- Fit $t(\approx p_T^2)$-spectra with $\frac{\mathrm{d}N}{\mathrm{d}t} = a\, e^{-kt}[1 + c(R(t) - 1)]$
  - k is slope parameter
  - Ratio $R(t) \equiv \frac{t\text{-spectrum with interference}}{t\text{-spectrum without interference}}$ from MC
  - Fit parameter c measures strength of interference
    - $c = 0$ corresponds to no interference
    - $c = 1$ is expected interference
- Different median impact parameters $\tilde{b}$
  - Topology data (no neutron tag): $\tilde{b} \approx 46$ fm
  - Minimum bias data (neutron tag): $\tilde{b} \approx 18$ fm

  $\Longrightarrow$ interference effects extend to larger p_T
- Energy dependence of ρ production amplitudes decreases interference effect at larger rapidities

Interference Effects in Coherent ρ Production

Measuring interference in run 2 Au $\times$ Au @ $\sqrt{s_{NN}} = 200$ GeV collisions

- Fit $t(\approx p_T^2)$-spectra with $\frac{\mathrm{d}N}{\mathrm{d}t} = a\,e^{-kt}[1 + c(R(t) - 1)]$
  - k is slope parameter
  - Ratio $R(t) \equiv \frac{t\text{-spectrum with interference}}{t\text{-spectrum without interference}}$ from MC
  - Fit parameter c measures strength of interference
    - $c = 0$ corresponds to no interference
    - $c = 1$ is expected interference
- Different median impact parameters $\tilde{b}$
  - Topology data (no neutron tag): $\tilde{b} \approx 46\,\mathrm{fm}$
  - Minimum bias data (neutron tag): $\tilde{b} \approx 18\,\mathrm{fm}$

  $\Longrightarrow$ interference effects extend to larger p_T
- Energy dependence of ρ production amplitudes decreases interference effect at larger rapidities

Interference Effects in Coherent ρ Production

Measuring interference in run 2 Au $\times$ Au @ $\sqrt{s_{NN}} = 200$ GeV collisions

- Fit $t(\approx p_T^2)$-spectra with $\dfrac{\mathrm{d}N}{\mathrm{d}t} = a\,e^{-kt}[1 + c(R(t) - 1)]$
  - k is slope parameter
  - Ratio $R(t) \equiv \dfrac{t\text{-spectrum with interference}}{t\text{-spectrum without interference}}$ from MC
  - Fit parameter c measures strength of interference
    - $c = 0$ corresponds to no interference
    - $c = 1$ is expected interference
- Different median impact parameters $\tilde{b}$
  - Topology data (no neutron tag): $\tilde{b} \approx 46\,\mathrm{fm}$
  - Minimum bias data (neutron tag): $\tilde{b} \approx 18\,\mathrm{fm}$

  $\Longrightarrow$ interference effects extend to larger p_T
- Energy dependence of ρ production amplitudes decreases interference effect at larger rapidities

Interference Effects in Coherent ρ Production

Run 2 minimum bias data $|y| < 0.5$

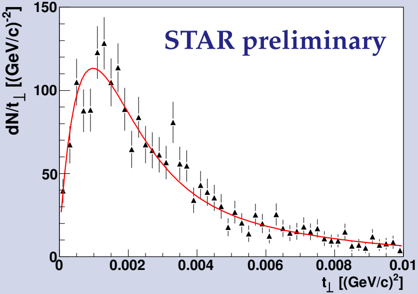

$c = 0.92 \pm 0.07_{\text{stat.}}, \chi^2/\text{ndf} = 45/47$

Run 2 topology data $0.05 < |y| < 0.5$

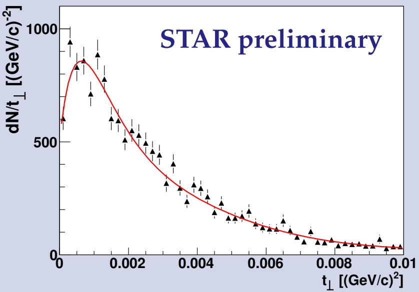

$c = 0.73 \pm 0.10_{\text{stat.}}, \chi^2/\text{ndf} = 53/47$

- Systematic effect due to imperfect trigger simulation

Outline

Photonuclear ρ Prod. in d $\times$ Au @ $\sqrt{s_{NN}} = 200\,\text{GeV}$

Asymmetric collision

- γ^* predominantly emitted by Au nucleus
- Topology data
  - Mainly $\gamma^*\,\mathrm{d} \to \rho\,\mathrm{d}$
  - Coherent coupling to entire deuteron
- Topology trigger in coincidence with ZDC neutron signal from deuteron breakup
  - Mainly $\gamma^*\,\mathrm{d} \to \rho\, pn$
  - Coupling to individual nucleons: "incoherent"
- Smaller radii: $R_\mathrm{d} \approx 2\,\text{fm}$, $R_N \approx 0.7\,\text{fm}$ $\implies$ ρ has larger p_T

Photonuclear ρ Prod. in d $\times$ Au @ $\sqrt{s_{NN}} = 200\,\text{GeV}$

Asymmetric collision

- γ^* predominantly emitted by Au nucleus
- Topology data
  - Mainly $\gamma^*\,\mathrm{d} \to \rho\,\mathrm{d}$
  - Coherent coupling to entire deuteron
- Topology trigger in coincidence with ZDC neutron signal from deuteron breakup
  - Mainly $\gamma^*\,\mathrm{d} \to \rho\,pn$
  - Coupling to individual nucleons: "incoherent"
- Smaller radii: $R_\mathrm{d} \approx 2\,\text{fm}$, $R_N \approx 0.7\,\text{fm}$ $\Longrightarrow$ ρ has larger p_T

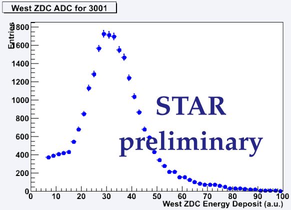

Neutron tagged data

Photonuclear ρ Prod. in d $\times$ Au @ $\sqrt{s_{NN}} = 200\,\text{GeV}$

Asymmetric collision

- γ^* predominantly emitted by Au nucleus
- Topology data
  - Mainly $\gamma^*\,\text{d} \to \rho\,\text{d}$
  - Coherent coupling to entire deuteron
- Topology trigger in coincidence with ZDC neutron signal from deuteron breakup
  - Mainly $\gamma^*\,\text{d} \to \rho\,pn$
  - Coupling to individual nucleons: "incoherent"
- Smaller radii: $R_\text{d} \approx 2\,\text{fm}$, $R_N \approx 0.7\,\text{fm}$ $\implies$ ρ has larger p_T

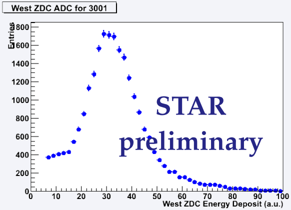

Neutron tagged data

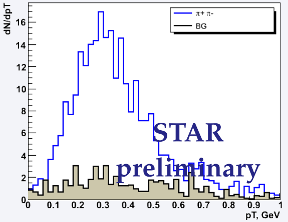

Photonuclear ρ Prod. in d $\times$ Au @ $\sqrt{s_{NN}} = 200$ GeV

t-spectrum for d-breakup ("incoherent")

- Exponential fit function: $\mathrm{d}N/\mathrm{d}t = a\, e^{-kt}$
- Slope parameter
  $k = 9.06 \pm 0.85_{\text{stat.}}\ \text{GeV}^{-2}$
  - Related to nucleon form factor
  - Similar to results from
    Au $\times$ Au @ $\sqrt{s_{NN}} = 200$ GeV :
    $k = 8.8 \pm 1.0_{\text{stat.}}\ \text{GeV}^{-2}$
    PR **C77**, 034910 (2008)
  - Compatible with ZEUS
    $k = 10.9 \pm 0.3_{\text{stat.}}\ {}^{+1.0}_{-0.5}{}_{\text{syst.}}\ \text{GeV}^{-2}$
    EPJ **C2**, 247 (1998)
- Downturn at low t
  - Not enough energy for d dissociation
  - Also seen in low-energy γd (SLAC 4.3 GeV Eisenberg *et al.*, NP **B104**, 61 (1976))

Neutron tagged data

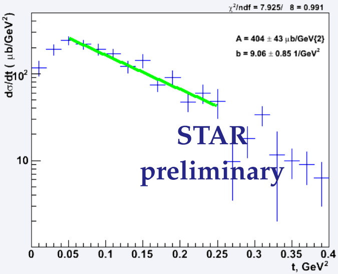

$t \approx t_\perp = p_T^2$

Photonuclear ρ Prod. in d $\times$ Au @ $\sqrt{s_{NN}} = 200$ GeV

t-spectrum for d-breakup ("incoherent")

- Exponential fit function: $\mathrm{d}N/\mathrm{d}t = a\,e^{-kt}$
- Slope parameter
  $k = 9.06 \pm 0.85_{\text{stat.}}\ \text{GeV}^{-2}$
  - Related to nucleon form factor
  - Similar to results from
    Au $\times$ Au @ $\sqrt{s_{NN}} = 200$ GeV :
    $k = 8.8 \pm 1.0_{\text{stat.}}\ \text{GeV}^{-2}$
    PR **C77**, 034910 (2008)
  - Compatible with ZEUS
    $k = 10.9 \pm 0.3_{\text{stat.}}\ {}^{+1.0}_{-0.5}{}_{\text{syst.}}\ \text{GeV}^{-2}$
    EPJ **C2**, 247 (1998)
- Downturn at low t
  - Not enough energy for d dissociation
  - Also seen in low-energy γd (SLAC 4.3 GeV Eisenberg *et al.*, NP **B104**, 61 (1976))

Neutron tagged data

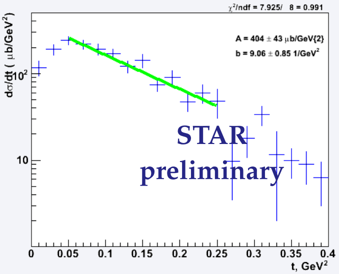

$$t \approx t_\perp = p_T^2$$

$\pi^+\pi^-\pi^+\pi^-$ Production in Au $\times$ Au @ $\sqrt{s_{NN}} = 200$ GeV

Photonuclear production with mutual nuclear excitation

- Run 4: 3.9 M multi-prong triggers
  - Coincident neutrons from nuclear breakup in both ZDCs
  - Low CTB multiplicity
  - Veto from large-tile BBCs

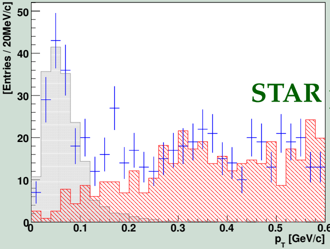

STAR preliminary

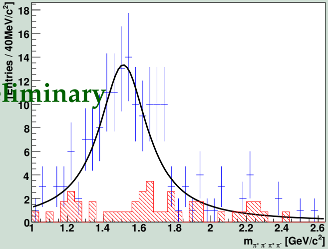

- Peak: 123 events at $m = (1510 \pm 20)$ MeV/c^2, $\Gamma = (330 \pm 45)$ MeV
- Could be $\rho(1450)$ and/or $\rho(1700)$

e^+e^--Pair Production in Au $\times$ Au @ $\sqrt{s_{NN}} = 200\,\text{GeV}$

Strong electromagnetic fields

- $Z\alpha \approx 0.6 \implies$ conventional perturbative calculations may be questionable
- Enrich collisions at small impact parameters (= stronger fields) by requiring mutual Coulomb excitation $2R_A < b \lesssim 30\,\text{fm}$

Run 2 minimum bias data

- Challenging measurement due to small acceptance
- Most $e^\pm$ produced at very low p_T
  - Reconstructible only at half solenoid field of 0.25 T
- $e^\pm$ identification via $\mathrm{d}E/\mathrm{d}x$ in TPC gas
  - Clean sample with PID efficiency close to 1 and minimum contaminations for $p_{e^\pm} < 130\,\text{MeV}/c$
- Limited statistics: 52 events

e^+e^--Pair Production in Au $\times$ Au @ $\sqrt{s_{NN}} = 200$ GeV

Strong electromagnetic fields

- $Z\alpha \approx 0.6 \implies$ conventional perturbative calculations may be questionable
- Enrich collisions at small impact parameters (= stronger fields) by requiring mutual Coulomb excitation $2R_A < b \lesssim 30\,\mathrm{fm}$

Run 2 minimum bias data

- Challenging measurement due to small acceptance
- Most $e^\pm$ produced at very low p_T
  - Reconstructible only at half solenoid field of 0.25 T
- $e^\pm$ identification via $\mathrm{d}E/\mathrm{d}x$ in TPC gas
  - Clean sample with PID efficiency close to 1 and minimum contaminations for $p_{e^\pm} < 130\,\mathrm{MeV}/c$
- Limited statistics: 52 events

e^+e^--Pair Production in Au $\times$ Au @ $\sqrt{s_{NN}} = 200$ GeV

Differential cross sections $d\sigma/dM_{e^+e^-}$ and $d\sigma/dp_T^{e^+e^-}$

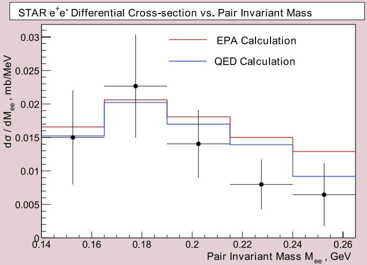

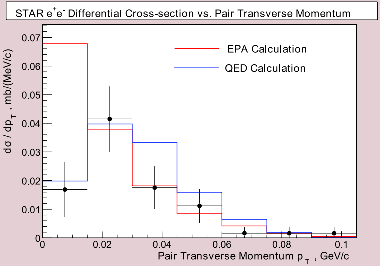

- Data compared with 2 models:
  - **EPA**: equivalent photon approach — PR **C70**, 031902 (2004)
    - Treats γ^* as real photons
    - Fails for lowest p_T bin ($p_T < 15$ MeV/c)
  - **QED**: lowest order QED calculation with simplified model for Coulomb excitation (GDR only) — Henken *et al.*, PR **C69**, 054902 (2004)
    - Describes data well

e^+e^--Pair Production in Au $\times$ Au @ $\sqrt{s_{NN}} = 200\,$GeV

Differential cross sections $d\sigma/dM_{e^+e^-}$ and $d\sigma/dp_T^{e^+e^-}$

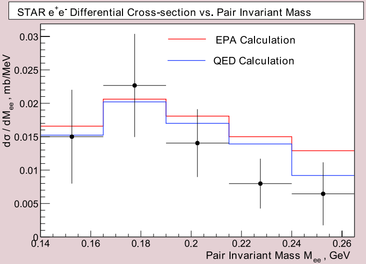

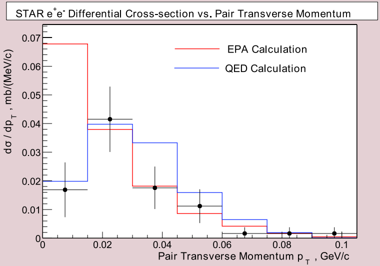

- Data compared with 2 models:
  - **EPA**: equivalent photon approach — PR **C70**, 031902 (2004)
    - Treats γ^* as real photons
    - Fails for lowest p_T bin ($p_T < 15$ MeV/c)
  - **QED**: lowest order QED calculation with simplified model for Coulomb excitation (GDR only) — Henken *et al.*, PR **C69**, 054902 (2004)
    - Describes data well

e^+e^--Pair Production in Au $\times$ Au @ $\sqrt{s_{NN}} = 200\,\mathrm{GeV}$

New QED calculation with realistic phenomenological treatment of Coulomb excitation

Baltz, PRL **100**, 062302 (2008)

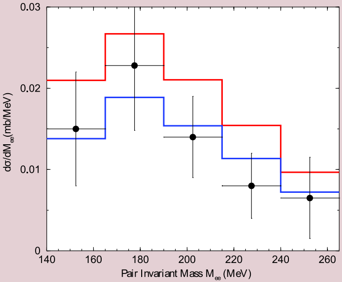

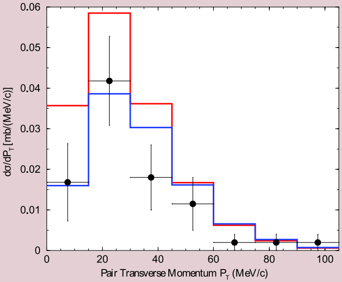

- **Lowest order QED**
  - Overshoots data
    $\sigma_{\text{QED}} = 2.34\,\text{mb}$ vs. $\sigma_{\text{exp}} = 1.6 \pm 0.2_{\text{stat.}} \pm 0.3_{\text{syst.}}\,\text{mb}$
- **Including higher order corrections**
  - Good agreement with data, $\sigma_{\text{QED}} = 1.67\,\text{mb}$

e^+e^--Pair Production in Au $\times$ Au @ $\sqrt{s_{NN}} = 200\,\mathrm{GeV}$

New QED calculation with realistic phenomenological treatment of Coulomb excitation

Baltz, PRL **100**, 062302 (2008)

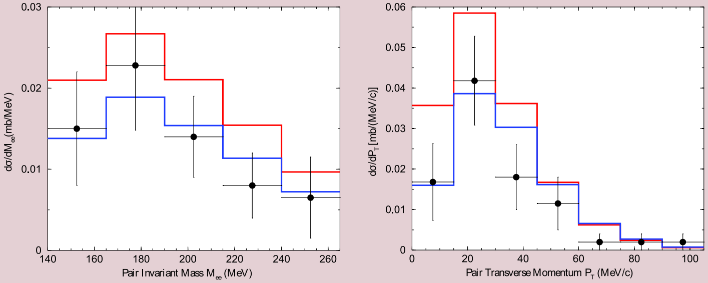

- **Lowest order QED**
  - Overshoots data
    $\sigma_{\mathrm{QED}} = 2.34\,\mathrm{mb}$ vs. $\sigma_{\mathrm{exp}} = 1.6 \pm 0.2_{\mathrm{stat.}} \pm 0.3_{\mathrm{syst.}}$ mb
- **Including higher order corrections**
  - Good agreement with data, $\sigma_{\mathrm{QED}} = 1.67\,\mathrm{mb}$

Conclusions

Summary

- Published new measurement of photonuclear ρ production in Au $\times$ Au @ $\sqrt{s_{NN}} = 200\,\text{GeV}$ collisions
  - Cross section agrees with theoretical models
  - Spin density matrix elements consistent with s-channel helicity conservation
- e^+e^--pair production in Au $\times$ Au @ $\sqrt{s_{NN}} = 200\,\text{GeV}$ collisions seems to deviate from lowest order QED calculations
- Work in progress:
  - STAR sees interference effects in ρ production close to expected level
  - Slope parameter for incoherent photonuclear ρ production in d $\times$ Au @ $\sqrt{s_{NN}} = 200\,\text{GeV}$ collisions compatible with results from Au $\times$ Au
  - Resonant $\pi^+\pi^-\pi^+\pi^-$ production in Au $\times$ Au @ $\sqrt{s_{NN}} = 200\,\text{GeV}$ collisions

Conclusions

Summary

- Published new measurement of photonuclear ρ production in Au $\times$ Au @ $\sqrt{s_{NN}} = 200$ GeV collisions
  - Cross section agrees with theoretical models
  - Spin density matrix elements consistent with s-channel helicity conservation
- e^+e^--pair production in Au $\times$ Au @ $\sqrt{s_{NN}} = 200$ GeV collisions seems to deviate from lowest order QED calculations
- **Work in progress:**
  - STAR sees interference effects in ρ production close to expected level
  - Slope parameter for incoherent photonuclear ρ production in d $\times$ Au @ $\sqrt{s_{NN}} = 200$ GeV collisions compatible with results from Au $\times$ Au
  - Resonant $\pi^+\pi^-\pi^+\pi^-$ production in Au $\times$ Au @ $\sqrt{s_{NN}} = 200$ GeV collisions

Conclusions

Outlook

- Run 7 Au $\times$ Au @ $\sqrt{s_{NN}} = 200\,\text{GeV}$ data soon ready for analysis
  - Expect increase in statistics to study rarer processes (J/ψ, $\pi^+\pi^-\pi^+\pi^-, \ldots$)
- STAR upgrades for 2009+
  - Time of flight detector
    - Replaces Central Trigger Barrel scintillators
    - Improved particle ID
    - Better trigger performance
  - Data acquisition upgrade
    - TPC can be read out with (1 kHz) at low dead-time
- LHC will open new horizons
  - Heavy flavors
  - Photon-photon collisions

Conclusions

Outlook

- Run 7 Au $\times$ Au @ $\sqrt{s_{NN}} = 200\,\text{GeV}$ data soon ready for analysis
  - Expect increase in statistics to study rarer processes (J/ψ, $\pi^+\pi^-\pi^+\pi^-, \ldots$)
- STAR upgrades for 2009+
  - Time of flight detector
    - Replaces Central Trigger Barrel scintillators
    - Improved particle ID
    - Better trigger performance
  - Data acquisition upgrade
    - TPC can be read out with (1 kHz) at low dead-time
- LHC will open new horizons
  - Heavy flavors
  - Photon-photon collisions

Conclusions

Outlook

- Run 7 Au $\times$ Au @ $\sqrt{s_{NN}} = 200\,\text{GeV}$ data soon ready for analysis
  - Expect increase in statistics to study rarer processes (J/ψ, $\pi^+\pi^-\pi^+\pi^-, \ldots$)
- STAR upgrades for 2009+
  - Time of flight detector
    - Replaces Central Trigger Barrel scintillators
    - Improved particle ID
    - Better trigger performance
  - Data acquisition upgrade
    - TPC can be read out with (1 kHz) at low dead-time
- LHC will open new horizons
  - Heavy flavors
  - Photon-photon collisions

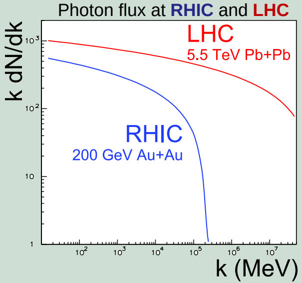

Outline

4 Backup slides
- Introduction
- Results on photonuclear ρ production in Au $\times$ Au collisions
- Other results

Ultra-Peripheral Heavy Ion Collisions (UPC) at STAR

- Nuclei surrounded by cloud of quasi-real virtual photons
- Number of photons large ($\propto Z^2$)
- Fast-moving heavy ions produce intense photon flux
  - Described by Weizsäcker-Williams approximation ("nuclear flashlight")
- Nuclear collisions: long range interaction via electromagnetic fields in addition to hadronic interactions
- Require $b > R_A + R_B$ to exclude (otherwise inseparable) hadronic interactions

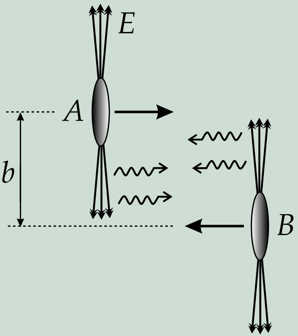

The Relativistic Heavy Ion Collider (RHIC) at BNL

Various particle species and collision energies

- Au + Au
  - $\sqrt{s_{NN}} = 19.6, 62.4, 130,$ and 200 GeV
- Cu + Cu
  - $\sqrt{s_{NN}} = 62.4$ and 200 GeV
- d + Au
  - $\sqrt{s_{NN}} = 200$ GeV
- polarized $p + p$
  - $\sqrt{s_{NN}} = 200$ and (future) 500 GeV

The STAR Experiment at RHIC

Solenoidal Tracker At RHIC (STAR)

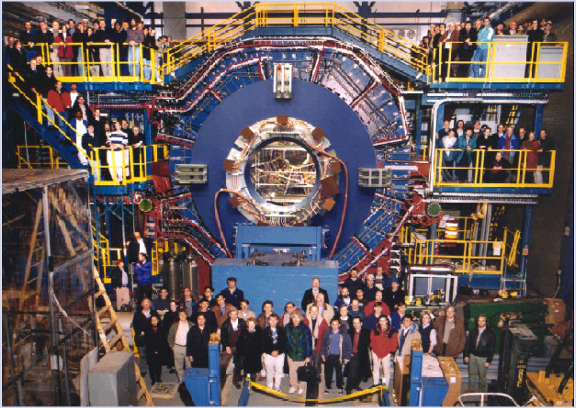

Big collaboration

- 533 scientists
- 52 institutes
- 12 countries

The STAR Experiment at RHIC

Trigger detectors

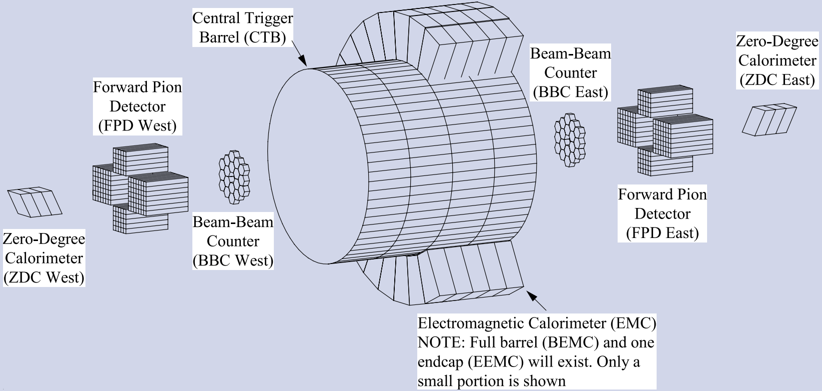

Ultra-Peripheral Relativistic Heavy Ion Collisions (UPC)

Three basic interaction processes

1. Photon-photon interactions

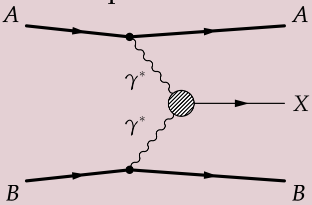

2. Photonuclear interactions

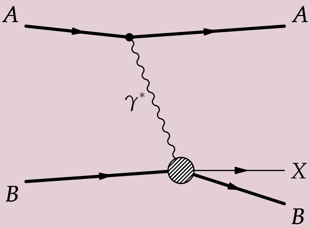

3. Nuclear breakup

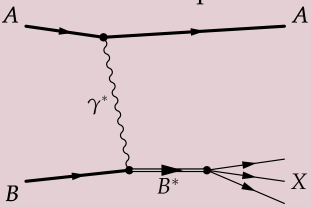

Ultra-Peripheral Relativistic Heavy Ion Collisions (UPC)

UPC kinematics for RHIC Au $\times$ Au @ $\sqrt{s_{NN}} = 200$ GeV and LHC Pb $\times$ Pb @ $\sqrt{s_{NN}} = 5500$ GeV

- Photons emitted coherently by whole nucleus
- Maximum photon energy in lab frame: $\omega_{\max} = \gamma_L \hbar c / R_A$
  $\omega_{\max} \approx 3\,\text{GeV}\ \ (\text{RHIC}), 80\,\text{GeV}\ \ (\text{LHC})$
- Photon-photon collisions: $\sqrt{s_{\gamma\gamma}^{\max}} = 2\gamma_L \hbar c / R_A$
  $\sqrt{s_{\gamma\gamma}^{\max}} \approx 6\,\text{GeV}\ \ (\text{RHIC}), 160\,\text{GeV}\ \ (\text{LHC})$
- Photonuclear interactions: $\sqrt{s_{\gamma N}^{\max}} = \sqrt{2\omega_{\max}\sqrt{s_{NN}}}$
  $\sqrt{s_{\gamma N}^{\max}} \approx 35\,\text{GeV}\ \ (\text{RHIC}), 950\,\text{GeV}\ \ (\text{LHC})$

UPC Triggers — Neutron tagging

Measuring nuclear breakup neutrons in Zero Degree Calorimeter (ZDC)

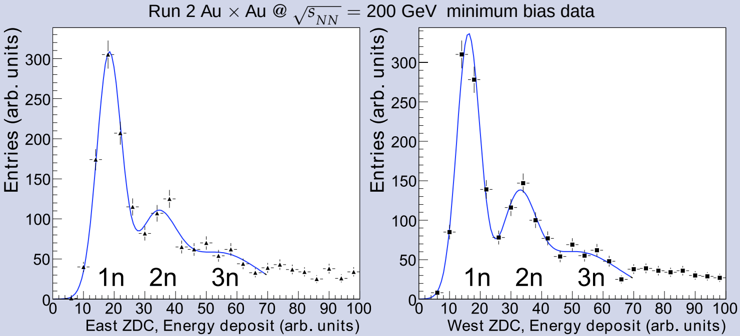

- ZDC acceptance for emitted neutrons close to 1
- Resolution good enough to see $1n, 2n, \ldots$ neutron peaks
  - Allows to select different excited states
- Neutron tag selects smaller impact parameters

UPC Triggers

Other triggers used at STAR

1. **Multi-prong trigger** (CTB and ZDC)
   - Coincident neutrons in both ZDCs
   - Low CTB multiplicity
   - Veto from large-tile BBCs
2. ***J/ψ* trigger** (CTB, ZDC, and BEMC)
   - Multi-prong trigger with additional calorimeter requirement
   - BEMC subdivided into 6 sectors
   - 2 high towers in non-neighboring BEMC sectors required

ρ Production Cross Section

Run 1 Au $\times$ Au @ $\sqrt{s_{NN}} = 130$ GeV data

p_T^ρ spectrum (Min. Bias)

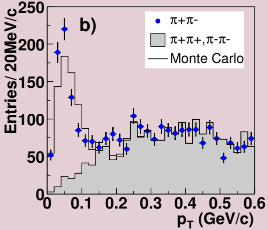

Rapidity distribution (Min. Bias)

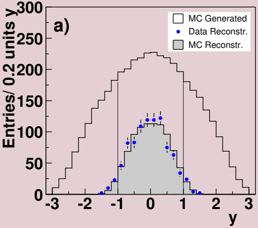

$d\sigma / dM_{\pi\pi}$ (Min. Bias)

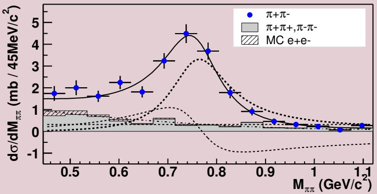

- Total cross section: $\sigma_{\text{tot}} = (460 \pm 220_{\text{stat.}} \pm 110_{\text{sys.}})$ mb
  PRL **89**, 272302 (2002)
- Theoretical prediction: $\sigma_{\text{tot}} = 350$ mb
  S. Klein *et al.*, PR **C60**, 014903 (1999)

Spin Structure of ρ Production Amplitudes

Extraction of spin density matrix elements from $\pi^+\pi^-$ angular distribution

$$\frac{1}{\sigma}\frac{d^2\sigma}{d\cos\theta\, d\phi} = \frac{3}{4\pi}\Bigg[\frac{1}{2}(1-r^{04}_{00}) + \frac{1}{2}(3r^{04}_{00}-1)\cos^2\theta - \sqrt{2}\,\mathfrak{Re}[r^{04}_{10}]\,\sin 2\theta\,\cos\phi - r^{04}_{1\,-1}\,\sin^2\theta\,\cos 2\phi\Bigg]$$

where $r^{04}_{ik} \equiv \dfrac{\rho^0_{ik} + \epsilon R\,\rho^4_{ik}}{1+\epsilon R}$, $R = \dfrac{\sigma_L}{\sigma_T}$ Schilling, Wolf NP **B61**, 381 (1973)

- θ is polar angle between beam direction and $\vec{p}_{\pi^+}$ in ρ RF
- ϕ is angle between ρ decay and production plane (w.r.t. beam)
- r^{04}_{00} represents probability that $\lambda_\rho = 0$ for $\lambda_{\gamma^*} = \pm 1$
- $\mathfrak{Re}[r^{04}_{10}]$ related to interference between helicity non-flip and single-flip
- $r^{04}_{1\,-1}$ related to interference between helicity non-flip and double-flip

Star Upgrades for 2009+

Time of Flight (ToF) Detector

- Replaces central trigger barrel
- Multi-gap resistive plate chambers (MRPC) using ALICE technology
- 23 000 channels (6 slats $\times$32 plates $\times$120 trays)
- Full coverage of TPC acceptance (2π in ϕ, $|\eta| < 1$)
- Intrinsic time resolution $\approx$ 85 ps

Upgrade of data acquisition (DAQ)

- New TPC front-end electronics based on ALICE's ALTRO chip
- Will permit trigger rates $\mathcal{O}(1\,\text{kHz}) \implies$ DAQ1000